Convergent structural alterations define SWItch/Sucrose NonFermentable (SWI/SNF) chromatin remodeler as a central tumor suppressive complex in pancreatic cancer

A. Hunter Shain[a], Craig P. Giacomini[a], Karen Matsukuma[a,b], Collins A. Karikari[b], Murali D. Bashyam[c], Manuel Hidalgo[d,e], Anirban Maitra[b], and Jonathan R. Pollack[a,1]

[a]Department of Pathology, Stanford University, Stanford, CA 94305; Departments of [b]Pathology and [d]Oncology, The Sol Goldman Pancreatic Cancer Research Center, The Johns Hopkins University School of Medicine, Baltimore, MD 21231; [c]Laboratory of Molecular Oncology, Centre for DNA Fingerprinting and Diagnostics, Nampally, Hyderabad 500001, India; and [e]Clinical Research Program, Centro Nacional de Investigaciones Oncológicas, E-28029 Madrid, Spain

Edited by Levi A. Garraway, Dana–Farber Cancer Institute, Boston, MA, and accepted by the Editorial Board December 15, 2011 (received for review September 8, 2011)

Defining the molecular genetic alterations underlying pancreatic cancer may provide unique therapeutic insight for this deadly disease. Toward this goal, we report here an integrative DNA microarray and sequencing-based analysis of pancreatic cancer genomes. Notable among the alterations newly identified, genomic deletions, mutations, and rearrangements recurrently targeted genes encoding components of the SWItch/Sucrose NonFermentable (SWI/SNF) chromatin remodeling complex, including all three putative DNA binding subunits (ARID1A, ARID1B, and PBRM1) and both enzymatic subunits (SMARCA2 and SMARCA4). Whereas alterations of each individual SWI/SNF subunit occurred at modest-frequency, as mutational "hills" in the genomic landscape, together they affected at least one-third of all pancreatic cancers, defining SWI/SNF as a major mutational "mountain." Consistent with a tumor-suppressive role, re-expression of SMARCA4 in SMARCA4-deficient pancreatic cancer cell lines reduced cell growth and promoted senescence, whereas its overexpression in a SWI/SNF-intact line had no such effect. In addition, expression profiling analyses revealed that SWI/SNF likely antagonizes Polycomb repressive complex 2, implicating this as one possible mechanism of tumor suppression. Our findings reveal SWI/SNF to be a central tumor suppressive complex in pancreatic cancer.

comparative genomic hybridization array | cancer gene discovery | tumor suppressor

Pancreatic ductal adenocarcinoma, more commonly known as pancreatic cancer, remains a leading cause of cancer deaths in the developed world (1, 2). Each year, the number of patients diagnosed with pancreatic cancer is nearly equal to the number that will die from the disease, underscoring the inadequacy of current therapies. Indeed, the overall 5-y survival rate is less than 5% (3). A more complete characterization of its molecular pathogenesis may suggest new avenues for targeted therapy.

Much has been learned of the molecular genetic alterations underlying pancreatic cancer (reviewed in 4, 5). Early events, identified in early precursor lesions [pancreatic intraepithelial neoplasia (PanIN)], include activational mutation (and/or amplification) of the *KRAS2* oncogene, occurring in 75–90% of pancreatic cancers, and inactivation of the *CDKN2A* ($p16^{INK4A}$) cell-cycle regulator in 80–95% of cases. Later events (identified in more advanced PanIN) include inactivation of the *TP53* tumor suppressor in 50–75% of pancreatic cancers, and loss of *SMAD4* (*DPC4*) in 45–55% of cases. SMAD4 is a downstream effector of TGF-β signaling, which is growth-inhibitory in epithelia (although it can also stimulate invasive phenotypes in cancer) (6). Loss of the TGF-β receptor (*TGFBR2*), although less common, also underscores the central role of the TGF-β signaling pathway. Nonetheless, the repertoire of molecular alterations underlying pancreatic cancer is incompletely understood, and efforts have generally lagged behind other major tumor types (7).

More recently, comparative genomic hybridization (CGH) and SNP arrays have facilitated the genome-wide survey of DNA copy number alterations in pancreatic cancer (8–10). Such studies have led to the identification of new pancreatic cancer genes, including, for example, *PAK4* (11, 12) and *GATA6* (13, 14), validating the utility of an agnostic, genome-wide approach.

In principle, genomic profiling with even higher resolution CGH/SNP arrays, along with characterization of larger sample numbers, should support the continued discovery of cancer genes. However, it might be supposed that the most important cancer genes, the high-incidence mutational "mountains" in the cancer genome landscape (15), have already been discovered. Here, by high-resolution genomic profiling of pancreatic cancers, integrated with mutational data, we uncover structural alterations converging on multiple subunits of the SWItch/Sucrose NonFermentable (SWI/SNF) chromatin remodeler, newly defining SWI/SNF as a major tumor suppressive complex in pancreatic cancer.

Results

Genomic Alterations in Pancreatic Cancer Target SWI/SNF Subunits. Previous genomic profiling studies of pancreatic cancer have been done at lower resolution and/or with fewer specimens (8, 9, 11, 16). Here, by high-resolution profiling (using Agilent 244K CGH arrays) of 70 pancreatic cancers (48 primary tumors engrafted in immunodeficient mice to enrich the epithelial fraction and 22 cancer cell lines), we observed the known aberrations, including amplification of *MYC* (8q24.21) and *KRAS* (12p12.1), and deletion of *TGFBR2* (3p24.1), *CDKN2A* (9p21.3), *MAP2K4* (17p12) (17), and *SMAD4* (18q21.2) (Fig. 1*A*). However, we were also able to identify numerous previously undescribed alterations, including recurrent gains at 9p13.3 and 19q13.2 (distinct from *AKT2*), and losses at 1p36.11 and 6p22.3 (*MBOAT1*) (Fig. 1*A* and Fig. S1) as well as at 6q25.3 (*ARID1B*), the starting point of our subsequent investigations.

ARID1B (BAF250B) encodes a putative DNA-binding subunit of the human SWI/SNF chromatin remodeling complex (18), a multiprotein complex that uses the energy of ATP to mobilize

Author contributions: A.H.S., C.P.G., M.D.B., and J.R.P. designed research; A.H.S., C.P.G., and K.M. performed research; C.A.K., M.H., and A.M. contributed new reagents/analytic tools; A.H.S., C.P.G., and J.R.P. analyzed data; and A.H.S. and J.R.P. wrote the paper.

The authors declare no conflict of interest.

This article is a PNAS Direct Submission. L.A.G. is a guest editor invited by the Editorial Board.

Data deposition: The microarray data reported in this paper have been deposited in the Gene Expression Omnibus (GEO) database, www.ncbi.nlm.nih.gov/geo (accession no. GSE26089).

[1]To whom correspondence should be addressed. E-mail: pollack1@stanford.edu.

See Author Summary on page 1370.

This article contains supporting information online at www.pnas.org/lookup/suppl/doi:10.1073/pnas.1114817109/-/DCSupplemental.

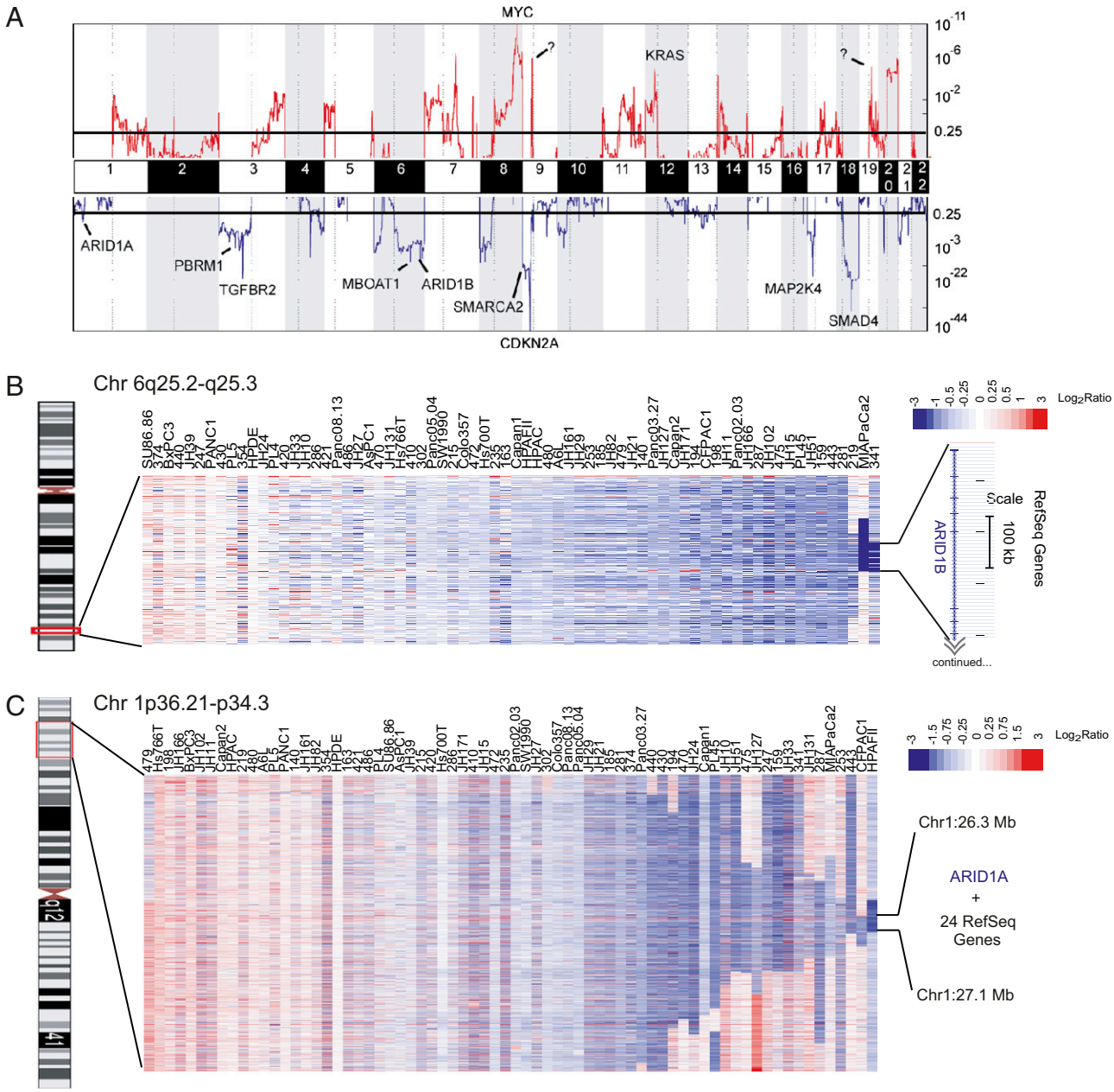

Fig. 1. Genomic DNA copy number alterations in pancreatic cancer. (*A*) GISTIC plot of the 70 pancreatic cancer specimens, integrating frequency and amplitude to identify significant amplifications (red) and deletions (blue) across the genome (ordered by chromosome). The threshold for significance is determined by the false discovery rate (q-value < 0.25). Known/candidate driver genes within selected peaks are indicated. Question marks identify newly identified loci that are depicted in greater detail in Fig. S1. (*B*) *ARID1B* is focally deleted in pancreatic cancer. The heat map shows gains and losses (red and blue, respectively; $\log_2$ ratio scale shown) for the 70 pancreatic cancer specimens across a subregion of 6q25.2-q25.3. CGH array probes are ordered by chromosome position, and samples are ordered by focality and amplitude of loss. Three focal deletions, including two homozygous deletions, of *ARID1B* are noted (far right). (*C*) Semifocal deletions span an ~870-kb region within 1p36.11, harboring *ARID1A* (along with 24 other genes).

nucleosomes to modulate transcription. SWI/SNF complexes have been characterized to function in diverse processes, including development and differentiation, and in control of the cell cycle (19). In our dataset, *ARID1B* was focally homozygously deleted in 2 of 70 samples, with broader, single-copy deletions spanning *ARID1B* in 74% of the other samples (Fig. 1*B*).

Interestingly, *ARID1A* (BAF250A), which encodes a mutually exclusive alternate subunit of SWI/SNF (18), resides within the recurrent deletion we identified at 1p36.11 (Fig. 1*C*). This gene-dense locus, heterozygously lost in 47% of samples, contains 25 genes. Mining published full exomic sequencing data of 24 pancreatic cancer cell lines and xenografts (8), only 2 of these 25 genes harbored DNA mutations. A single missense mutation was found in *AIM1L*, whereas two deleterious mutations, one nonsense and one small deletion (leading to a frameshift), were identified in *ARID1A* (Table 1). By transcriptome sequencing [paired-end RNA sequencing (RNAseq)] of pancreatic cancer cell lines, we identified an additional deleterious *ARID1A* mutation: a nonsense mutation in Hs766T cells (Table 1 and Fig. S2*A*). We also identified a genomic rearrangement consistent with an internal duplication of *ARID1A* exons 2–4 in PANC1 cells (Table 1 and Fig. S2*B*). The mutational data therefore implicate *ARID1A* as the likely target of 1p36.11 deletion.

Table 1. Components of SWI/SNF are mutated in pancreatic cancer

Gene name (transcript accession identification)	Tumor/cell line	Amino acid	Mutation type	Source	Frequency
ARID1A (CCDS285.1)	A32-1	p.R1276X	Nonsense	Jones et al. (8)	8% (2 of 25)
	185	fs	INDEL		
	Hs766T	p.Q538X	Nonsense	RNAseq	
	Panc1	In-frame	Rearrangement		
PBRM1 (CCDS2859.1)	PL45	p.R502X	Nonsense (homozygous)	Jones et al. (8)	8% (2 of 25)
	140	p.P1269L	Missense		
SMARCA4 (CCDS12253.1)	A10.7	p.Q1196X	Nonsense (homozygous)	Jones et al. (8)	8% (2 of 25)
	TS 0111	Splice site	Splice site		
	Hs700T	fs	Frameshift (homozygous)	Wong et al. (21)	18% (2 of 11)
	SU86.86	p.Q160R	Missense		
	Panc1	fs	Rearrangement	RNAseq	

In addition to ARID1A or ARID1B, the human SWI/SNF complex contains either of two mutually exclusive enzymatic ATPase subunits: SMARCA2 (BRM) or SMARCA4 (BRG1) (19, 20). Furthermore, in one version of the complex, PBRM1 (BAF180) replaces ARID1A/1B (although only in association with SMARCA4). SWI/SNF complexes also contain 8–10 other "core" and accessory subunits, or BRM- or BRG1-associated factors (BAFs) (19, 20). We therefore sought to determine whether other SWI/SNF components, in addition to ARID1A and ARID1B, might be targeted by genomic deletion/mutation.

Located on chromosome 3p, *PBRM1* was deleted frequently (Fig. 1*A*). These were nearly all broad events, likely driven, in part, by loss of *TGFBR2* located on the same arm. However, in a single xenograft, a focal homozygous deletion was detected ~10 kb upstream of the *PBRM1* transcription start site (Fig. 2*A*). Notably, from microarray expression data, PBRM1 transcript levels in this specimen were the third lowest of 50 xenografts profiled (Fig. 2*B*), suggesting that the deletion likely interferes with PBRM1 expression. Mining DNA sequencing data (8), *PBRM1* was mutated in 8% of samples (Table 1). One of these mutations was a homozygous nonsense mutation occurring in a cell line (PL45) also in our profiling analysis. Both transcript and protein levels were undetectable in this sample (Fig. 2 *B* and *C*).

Of the SWI/SNF ATPase subunits, *SMARCA4* (located at 19p13.2) exhibited a focal homozygous deletion at the 5′ end of the gene in a single sample (Capan2); the deletion was confirmed using data from an independent SNP array platform (16) (Fig. 2*D*). This deletion ablated both the transcript and protein (Fig. 2 *E* and *F*). From sequencing studies (8, 21), *SMARCA4* was also found mutated in 4 (11%) of 35 pancreatic cancer samples (Table 1). A cell line (Hs700T) harboring a homozygous frameshift mutation, and also included in our dataset, showed no detectable SMARCA4 protein (Fig. 2*F*). Our paired-end RNAseq analysis also identified an internal duplication of *SMARCA4* exons 25–28 (resulting in a frameshift with early termination) in PANC1 cells (Figs. 2*G*, Fig. S2*C*, and Table 1); this rearrangement was associated with loss of the transcript and protein (Fig. 2 *E* and *F*).

The alternate ATPase subunit, *SMARCA2* (at 9p24.3), showed no mutations, but frequent single-copy deletions spanned the gene in our dataset (Figs. 1*A* and 2*H*). Analyzing published high-resolution SNP array data from seven pancreatic cancer cell lines not included in our study (16), we identified a homozygous deletion of *SMARCA2* in one cell line (Hup-T4) and a focal single-copy deletion of the 3′ end of *SMARCA2* in another cell line (YAPC) (Fig. 2*H*).

We also assessed the genomic copy number and mutational status of other known BAF genes, including *SMARCB1* (SNF5), *SMARCC1* (BAF155), *SMARCC2* (BAF170), *SMARCD1* (BAF60a), *SMARCD2* (BAF60b), *SMARCD3* (BAF60c), *SMARCE1* (BAF57), *ACTL6A* (BAF53a), *ACTL6B* (BAF53b), and *ARID2* (BAF200). Using the conservative criterion that at least one genomic aberration must be unequivocally focal, other components of the complex did not appear to be selectively deleted, nor have any mutations been reported (8). It remains possible that such alterations occur at a lower frequency, but their detection would require analysis of larger sample numbers.

To survey SWI/SNF abnormalities at the protein level more systematically, we performed Western blot analysis of the ATPase (SMARCA2 and SMARCA4) and putative DNA-binding (ARID1A, ARID1B, and PBRM1) subunits across the panel of pancreatic cancer cell lines (Fig. 3). In several cell lines, deficiency of a single SWI/SNF subunit was identified, which was explainable in most cases by an underlying genomic alteration (deletion, rearrangement, or mutation; annotated in Fig. 3). One cell line (MIAPaCa2) was deficient in two SWI/SNF subunits. Reduced (but not absent) expression of one or more subunits was also apparent in several cell lines. For example, PANC1 showed reduced levels of SMARCA2 and PBRM1 (in addition to SMARCA4 deficiency and *ARID1A* rearrangement), suggesting that multiple subunits had likely been targeted for loss.

Functional and Mechanistic Characterization of SWI/SNF as a Tumor Suppressor. The finding of multiple deletions, rearrangements, and inactivating mutations in the enzymatic and putative DNA-binding subunits of the SWI/SNF complex strongly implies a tumor-suppressive role. To obtain direct functional evidence, we examined the effect of re-expressing SMARCA4 (the more frequently mutated of the enzymatic subunits) in SMARCA4-deficient pancreatic cancer cell lines (PANC1 and Hs700T). Consistent with a tumor-suppressive function, re-expression of SMARCA4 (by retroviral transduction) in both PANC1 and Hs700T cells, confirmed by Western blot analysis (Fig. 4*A*), led to significantly reduced cell line growth ($P < 0.01$; Fig. 4*B* and Fig. S3*A*). In contrast, overexpression of SMARCA4 in a human pancreatic ductal epithelial (HPDE) cell line (22) without SWI/SNF deficiency had no perceptible growth phenotype (Fig. 4 *A* and *B* and Fig. S3*A*), precluding any nonspecific toxicity of SMARCA4 overexpression. Interestingly, expression of an enzymatically dead SMARCA4 mutant (K798R), characterized to be a dominant-negative mutant (23–26), promoted cell growth in PANC1 cells but inhibited growth in Hs700T cells, whereas it had only a nominal effect in HPDE cells (Fig. 4 *A* and *B* and Fig. S3*A*). We chose to characterize the PANC1 system further based on the disparate phenotypes observed with re-expression of SMARCA4 and SMARCA4 (K798R).

Concordant with the above cell growth results, we noted that the re-expression of SMARCA4 in PANC1 cells was lost after

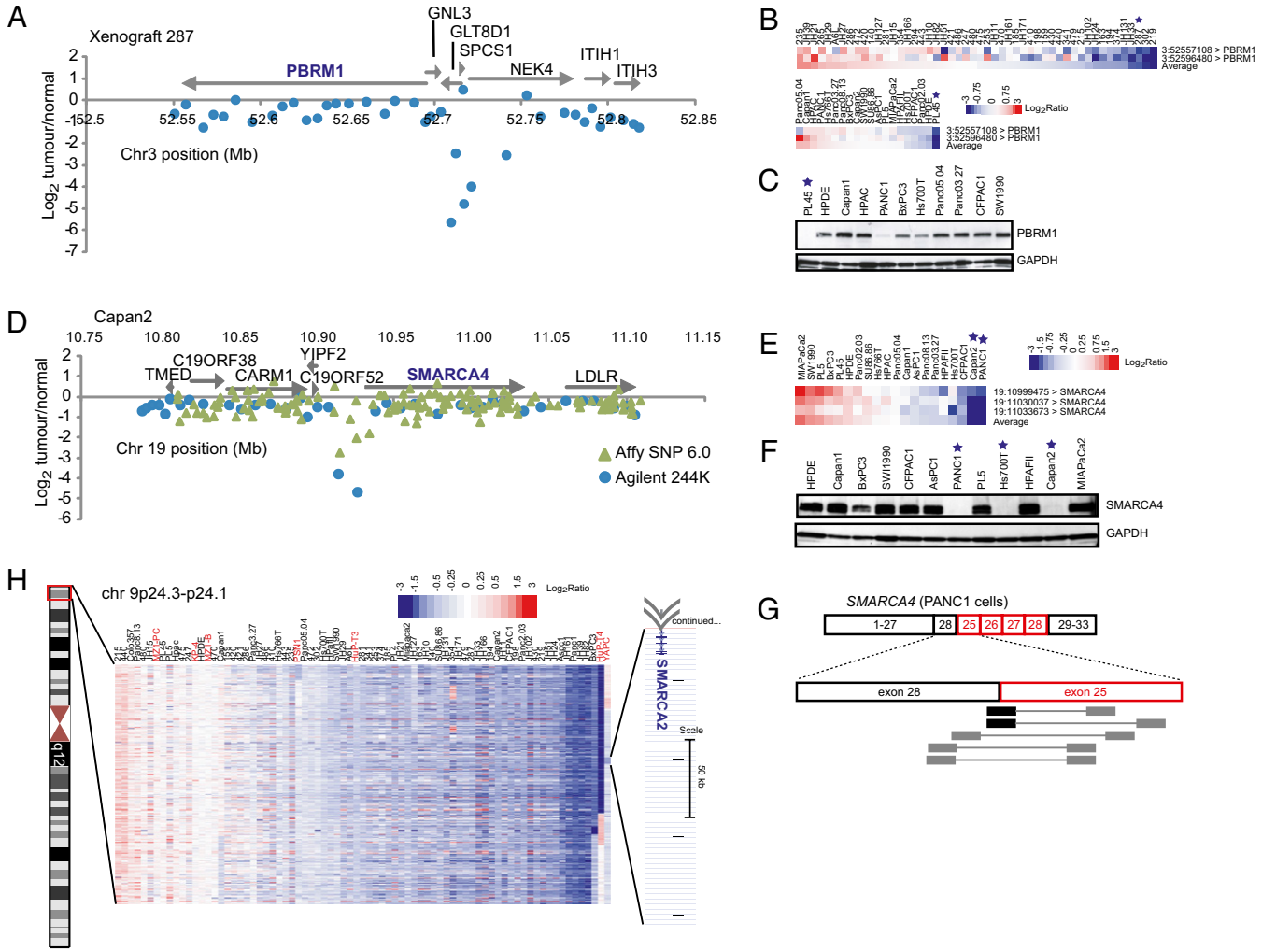

Fig. 2. Deletions target SWI/SNF genes *PBRM1*, *SMARCA4*, and *SMARCA2* in pancreatic cancer. (*A*) Array CGH profile of xenograft 287 across a subregion of 3p21.1 identifies a homozygous deletion ~10 kb upstream of *PBRM1* transcriptional start. Tumor/normal $\log_2$ ratios of CGH array probes are plotted by chromosome Mb position. (*B*) Reduced PBRM1 expression in xenograft 287 and in the PL45 cell line (harboring a homozygous nonsense mutation); samples are identified by a star. Transcript levels are depicted by a $\log_2$ ratio scale, separately median-centered for xenografts (*Upper*) and cell lines (*Lower*), and shown for two array probes and ordered by their average. (*C*) PBRM1 protein is undetected by Western blot in PL45 (star), among a panel of pancreatic cell lines assayed. GAPDH serves as a loading control. (*D*) Homozygous deletion overlapping the 5′ end of *SMARCA4* is identified in Capan2 by high-resolution CGH array (probes represented by blue dots) and by SNP array (green triangles) (16). (*E*) Reduced SMARCA4 transcript in Capan2 and PANC1 cells. (*F*) SMARCA4 protein is undetected by Western blot in Capan2, Hs700T, and PANC1 cells. (*G*) Schematic depiction of RNAseq-identified internal duplication of *SMARCA4* exons 25–28 in PANC1 cells (detailed further in Fig. S2*C*). (*H*) Heat map of copy number alterations across a subregion of 9p24.3-p24.1 reveals focal deletions targeting *SMARCA2* (far right). Samples labeled in red text are included from publicly available SNP array data (16) (*Experimental Procedures*).

30 d in culture, whereas expression of the K798R enzymatic mutant was retained (Fig. 4*C*). Furthermore, transfection of SMARCA4 into PANC1 cells led to reduced clonogenicity (colony growth on plastic) compared with the enzymatic mutant ($P < 0.001$; Fig. S3*D*). Lastly, SMARCA4 re-expression induced a striking morphological change, with many larger and flatter appearing cells (Fig. S3*B*). The morphological change was suggestive of cellular senescence, which we confirmed by finding increased senescence-associated β-galactosidase staining (Fig. 4*D* and Fig. S3*C*).

To complement the re-expression studies, we also analyzed the effects of RNAi-mediated knockdown (mimicking deletion) of SWI/SNF subunits in nontumorigenic cell lines with intact SWI/SNF. For these experiments, we chose HPDE cells and HaCaT keratinocytes (27), the latter because of the paucity of available nontumorigenic pancreatic epithelial lines and because of its being previously characterized to have intact, functional SWI/SNF complexes (28). Consistent with a tumor-suppressive function, knockdown of ARID1B promoted the growth factor-independent growth (a property of cancer cells) of HPDE cells ($P < 0.01$; Fig. S4 *A* and *B*), as well as the growth of HaCaT cells in complete medium [with 10% (vol/vol) FBS] ($P < 0.01$; Fig. S4 *C* and *D*). In contrast, knockdown of ARID1A and SMARCA4 either did not affect cell growth (Fig. S5*A*) or reduced cell growth (Fig. S5 *B*–*D*), suggesting some measure of context dependency. In that regard, we note that inactivation of SMARCB1 (SNF5), a SWI/SNF subunit and a bona fide tumor suppressor (lost in rhabdoid tumors) (19), was previously shown to up-regulate a proliferative gene-expression signature yet, paradoxically, to reduce the proliferation of mouse embryo fibroblasts (MEFs) (29).

To gain additional mechanistic insight, we sought to analyze the gene-expression changes occurring with ARID1A, ARID1B, and SMARCA4 knockdown in HPDE cells. Of particular interest would be gene expression patterns shared across all three SWI/SNF subunit knockdowns. Notably, knockdown of

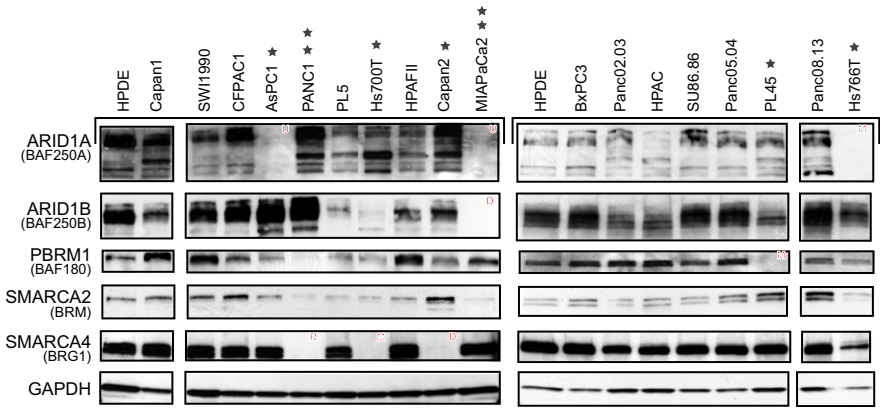

Fig. 3. SWI/SNF subunit expression in pancreatic cancer lines. Western blots of ARID1A, ARID1B, PBRM1, SMARCA2, and SMARCA4, done as two separate blots (bracketed). HPDE lysates appear on both blots to facilitate comparison, and GAPDH serves as a loading control. Cell lines with SWI/SNF subunit complete deficiency are identified by a star. Underlying genomic alterations/mutations are annotated as follows: D, homozygous deletion; M, deleterious point mutation (Table 1); R, internal gene rearrangement (detailed in main text); U, undetermined.

ARID1A, ARID1B, and SMARCA4 in HPDE cells was each associated with the significant down-regulation of gene sets that are themselves up-regulated with knockdown of Enhancer of Zeste Homolog 2 (EZH2) or histone deacetylase (HDAC) (Table 2). EZH2 is the catalytic subunit of Polycomb repressive complex 2 (PRC2), a histone methyltransferase that functions in conjunction with HDACs to maintain a transcriptional-repressive state (30–32). Our findings suggest that SWI/SNF might oppose PRCs in pancreatic epithelial cells, consistent with a recent report examining SMARCB1 (SNF5) in rhabdoid tumors and murine lymphomas (33).

Discussion

The SWI/SNF chromatin remodeling complex has known functions consistent with tumor suppression, including mediating RB1 regulation of the cell cycle (by repressing E2F targets) (19, 20, 34). Some SWI/SNF subunit genes have also been reported to show loss of heterozygosity, or altered protein levels in cancers

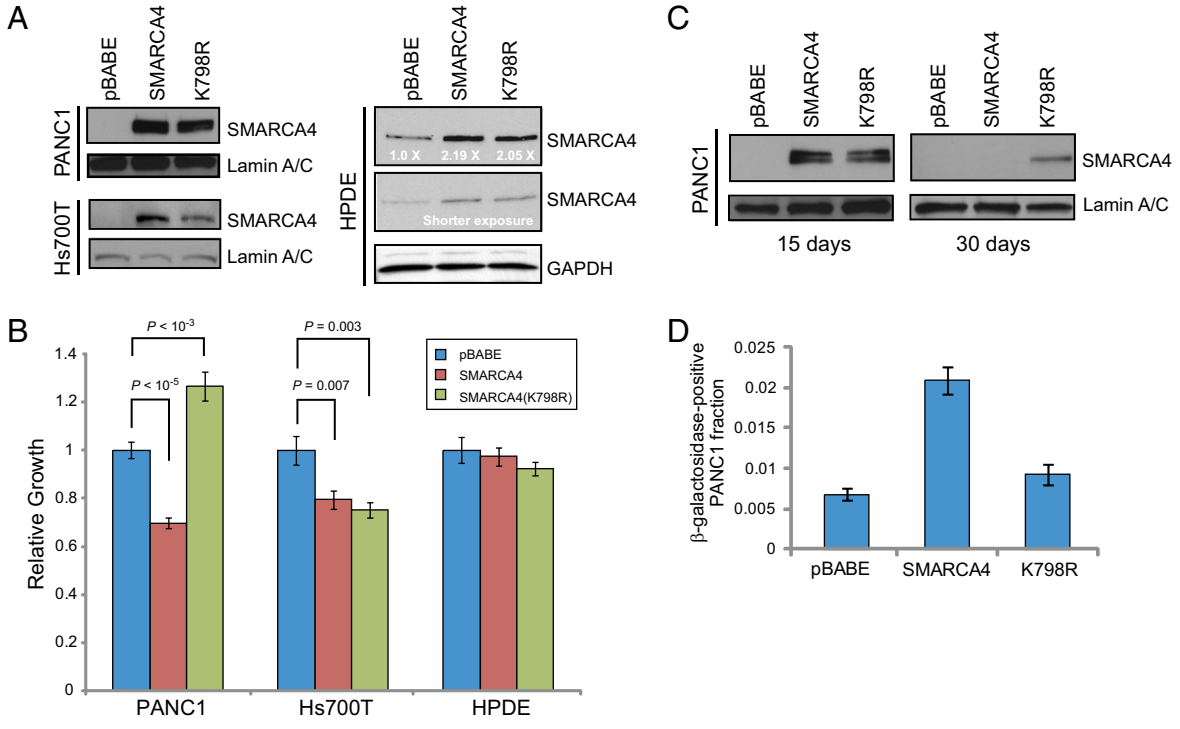

Fig. 4. Re-expression of SMARCA4 in deficient lines reduces cell growth. (*A*) Western blot confirming re-expression of transduced SMARCA4 or SMARCA4 (K798R) mutant in PANC1 and Hs700T cells, and overexpression in HPDE cells (protein levels quantified relative to pBABE empty vector). Lamin A/C and GAPDH serve as loading controls. (*B*) Cell growth of PANC1, Hs700T, and HPDE cells 5 d after transduction of SMARCA4 or SMARCA4 (K798R), quantified relative to pBABE empty vector. Error bars represent SDs. *P* values (two-sided Student *t* test) are indicated. (*C*) Western blot of PANC1 cells 15 and 30 d after transduction of empty vector (pBABE), SMARCA4, or SMARCA4 (K798R) shows selective loss of SMARCA4 expression with prolonged cell culture. Blots shown are representative of independently replicated experiments. (*D*) Senescence-associated β-galactosidase staining of transduced PANC1 cells, confirming increased senescence with SMARCA4 re-expression.

Table 2. Polycomb-related gene sets enriched with SWI/SNF subunit knockdown*

siRNA target	Gene set	Description	Enrichment *P* value
ARID1A	NUYTTEN EZH2 TARGETS UP	Genes up-regulated in PC3 cells (prostate cancer) after knockdown of EZH2 by RNAi	4.55E-11
	SENESE HDAC1 TARGETS UP	Genes up-regulated in U2OS cells (osteosarcoma) on knockdown of HDAC1 by RNAi	9.13E-09
	SENESE HDAC3 TARGETS UP	Genes up-regulated in U2OS cells (osteosarcoma) on knockdown of HDAC3 by RNAi	2.03E-07
	SENESE HDAC2 TARGETS UP	Genes up-regulated in U2OS cells (osteosarcoma) on knockdown of HDAC2 by RNAi	9.80E-05
ARID1B	NUYTTEN EZH2 TARGETS UP	Genes up-regulated in PC3 cells (prostate cancer) after knockdown of EZH2 by RNAi	<10E-12
	SENESE HDAC3 TARGETS UP	Genes up-regulated in U2OS cells (osteosarcoma) on knockdown of HDAC3 by RNAi	3.49E-08
	SENESE HDAC1 AND HDAC2 TARGETS UP	Genes up-regulated in U2OS cells (osteosarcoma) on knockdown of both HDAC1 and HDAC2 by RNAi	4.02E-06
	KONDO EZH2 TARGETS	Genes up-regulated in PC3 cells (prostate cancer) after EZH2 knockdown by RNAi	5.34E-06
SMARCA4	NUYTTEN EZH2 TARGETS UP	Genes up-regulated in PC3 cells (prostate cancer) after knockdown of EZH2 by RNAi	<10E-12
	SENESE HDAC3 TARGETS UP	Genes up-regulated in U2OS cells (osteosarcoma) on knockdown of HDAC3 by RNAi	1.66E-11
	KONDO EZH2 TARGETS	Genes up-regulated in PC3 cells (prostate cancer) after EZH2 knockdown by RNAi	6.49E-07

*Gene sets shown are significantly enriched among the top 200 genes down-regulated with SWI/SNF subunit knockdown in HPDE cells.

[including pancreatic cancer (35, 36)]. Until recently, however, *SMARCB1* (SNF5, a SWI/SNF accessory subunit) has been described as the only bona fide tumor suppressor (19) because of its homozygous inactivation in most rhabdoid tumors. Very recent studies have now also reported *ARID1A* to be mutated in about half of ovarian clear cell carcinomas (37, 38) and *PBRM1* in ~40% of renal clear cell carcinomas (39).

Here, by high-resolution array CGH, integrated with gene-expression profiling and exon and transcriptome sequencing, we have identified structural alterations and mutations in pancreatic cancer that converge on all five of the ATPase and putative DNA-binding subunits of the SWI/SNF complex. Counting only focal deletions and deleterious mutations, inactivation of each individual subunit occurs at modest frequency (2–10%). However, taken together, genomic aberrations target the SWI/SNF complex in at least 34% of cases (Fig. 5, Table S1, and *SI Text*), defining SWI/SNF as a central tumor-suppressive complex in pancreatic cancer. Western blot analysis of SWI/SNF subunits, confined to the cell lines, reveals subunit deficiencies in a comparable fraction of cases [7 (13%) of 18 lines; Fig. 3]. Notably, however, these estimates are conservative, ignoring, for example, cases with broader deletions or reduced (but not absent) protein levels; the true frequency of SWI/SNF abnormalities is likely to be substantially higher.

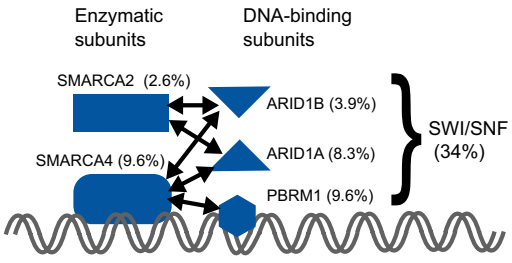

Fig. 5. Schematic summary of SWI/SNF subunit alterations in pancreatic cancer. Enzymatic and putative DNA-binding subunits are shown, with the arrows denoting possible pairings within SWI/SNF complexes. Subunit-specific (and total) frequencies of deletion/mutation are indicated. Details of the analysis are provided in *SI Text*.

In many instances, SWI/SNF subunit deletions or mutations occur as homozygous alterations, indicative of classic tumor suppressors (requiring loss of both alleles). However, a high frequency of single-copy deletions (e.g., at the *ARID1A* locus; Fig. 1*C*) suggests the possibility of haploinsufficiency, where loss of one allele may compromise tumor suppression. In most instances, alterations of SWI/SNF subunits are mutually exclusive [i.e., only a single subunit is affected (by genomic alterations and/or protein deficiency) in any given pancreatic cancer]. However, two cell lines (PANC1 and MIAPaCa2) harbor alterations of two different subunits, suggesting that loss of multiple subunits may further compromise the complex. Indeed, given the combinatorial complexity of SWI/SNF components, with alternative DNA-binding and enzymatic subunits all expressed in pancreatic epithelial cells (HPDE cells; Fig. 3), it would seem difficult to predict how subunit loss (or haploinsufficiency) might alter the stoichiometry and functions of residual SWI/SNF complexes.

To characterize the functional consequence of SWI/SNF alteration in pancreatic cancer, we first re-expressed SMARCA4 in two different SMARCA4-deficient pancreatic cancer cell lines. Consistent with a tumor-suppressive function, SMARCA4 re-expression led to reduced cell line growth (but not in HPDE cells, excluding nonspecific toxicity) that was at least, in part, attributable to increased cellular senescence. Intriguingly, re-expression of an enzymatically inactive, dominant-negative SMARCA4 mutant led to disparate phenotypes, with increased growth in PANC1 cells and decreased growth in Hs700T cells. PANC1 cells harbor structural alterations in multiple components of SWI/SNF, whereas Hs700T cells are deficient only in SMARCA4. Thus, we can speculate that Hs700T cells might be more dependent on residual (SMARCA2-containing) SWI/SNF complexes, which would be compromised by the dominant-negative SMARCA4 mutant. Future studies should provide clarification.

To complement the re-expression studies, we also knocked down (simulating deletion) individual SWI/SNF subunits (ARID1A, ARID1B, and SMARCA4) in nontumorigenic cell

lines with intact SWI/SNF complexes. In some contexts, subunit knockdown enhanced cell growth (consistent with tumor-suppressive function, most notably for ARID1B), whereas in other contexts, it had no effect or even reduced growth. As noted earlier, knockdown of SMARCB1 (SNF5), a bona fide tumor suppressor, also paradoxically inhibits cell proliferation (in MEF cells, likely by activating cell-cycle checkpoints) (29), underscoring the context dependency of SWI/SNF function. Nevertheless, the genetic data (recurrent inactivating deletions and mutations) combined with the re-expression experiments provide strong support for a tumor-suppressive role of SWI/SNF in pancreatic cancer.

To gain additional mechanistic insight, we profiled the gene-expression changes occurring with SWI/SNF subunit (ARID1A, ARID1B, and SMARCA4) knockdown in pancreatic cells. A theme to emerge from these studies is an apparent SWI/SNF antagonism of PRCs. SWI/SNF and Polycomb group (PcG) proteins have long been known to play antagonistic roles during development (40–42), but this observation was recently extended to oncogenesis (33). Furthermore, emerging evidence suggests that EZH2 (the enzymatic subunit of PRC2) is oncogenic; EZH2 is up-regulated in several different cancer types, and its expression maintains or enhances tumor cell growth (32). Thus, it is possible that in pancreatic cancer, SWI/SNF alterations lead to imbalanced PRC2 activity, with resultant tumor-promoting consequence. Our findings provide a starting point for further exploration of this mechanistic insight.

In pancreatic cancers, we found that genomic alterations targeted multiple subunits of SWI/SNF. We therefore wondered whether such might also be the case in other SWI/SNF- dependent cancers. In ovarian clear cell carcinoma, *ARID1A* was recently found to be mutated in ~50% of cases (37, 38). One of those studies (38) reported full-exome sequencing data from eight samples (of which *ARID1A* was mutated in 5 tumors). Although the power is limited in this discovery screen, mutations are also apparent in *ARID1B* and *SMARCA4* (each in a single tumor) (Table S2). Similarly, although *PBRM1* is predominately targeted in renal clear cell carcinoma, Varela et al. (39) noted a single mutation in *ARID1A*. Thus, it appears likely that SWI/SNF subunits are more broadly targeted, although certain subunit genes (and mechanisms of inactivation) may predominate in specific cancers. The extent to which SWI/SNF components are targeted in other common epithelial tumor types remains to be explored.

In summary, by genomic profiling (integrated with transcriptome profiling/sequencing and mutational analysis), we have identified SWI/SNF to be a major tumor-suppressive complex in pancreatic cancer, perhaps, at least by frequency, as important as TP53. How could such a significant tumor suppressor have eluded previous discovery? To borrow a metaphor from Vogelstein and colleagues (15), each SWI/SNF subunit gene individually represents only a "hill" in the genomic mutational landscape. Only when recognized together do they amass to a mutational "mountain." More broadly, therefore, our findings underscore the importance of integrative analysis in discovering key complexes and pathways in human cancers. In conclusion, we have identified SWI/SNF as a central tumor-suppressive complex in pancreatic cancer, providing unique insight and potential therapeutic avenues for this deadly disease.

Experimental Procedures

Genomic Profiling. Tumor xenografting, which effectively enriches the cancer epithelial fraction for DNA analysis, was done as previously described (43). Genomic DNA and RNA were isolated using the Qiagen DNA/RNA Allprep kit. Genomic profiling was done using Agilent 244K CGH arrays. Test DNA was labeled with Cy5, and sex-matched reference DNA (pooled from 8 individuals) was labeled with Cy3. Labeling and hybridization were done according to the manufacturer's instructions (Agilent). Fluorescence intensities were extracted, normalized, and mapped onto the genome (build 18) using Agilent software. GISTIC (Genomic Identification of Significant Targets in Cancer) (44) was implemented using the GenePattern platform (45). The array CGH dataset is available in the Gene Expression Omnibus (GEO) database (accession no. GSE26089). Publicly available (16) Affymetrix SNP 6.0 array data for seven cell lines not included in our Agilent 244K CGH study were used to supplement the data reported here in Fig. 2*H*. To integrate and visualize the data, we mapped each Affymetrix SNP 6.0 probe to the nearest corresponding probe on the Agilent 244K CGH array platform.

Expression Profiling. Expression profiling of pancreatic cancer cell lines and xenografts was done using Agilent 44K Gene Expression arrays. RNA was labeled using the Agilent Quick Amp Labeling Kit. Test RNA was labeled with Cy5, and a universal reference RNA (pooled from 11 diverse cell lines) was labeled with Cy3. Expression profiling of HPDE cells (for siRNA experiments) was done using Affymetrix Human Gene 1.0 ST Arrays. Samples were hybridized according to the manufacturer's instructions, and fluorescence intensities were extracted and normalized using the manufacturer's software. The microarray expression data are also available in the GEO database (accession no. GSE26089).

Transcriptome Sequencing. Paired-end RNAseq was done using Illumina kits and reagents. Briefly, mRNA was fragmented, reverse-transcribed, and adapter-ligated, from which size-selected (300 bp) sequencing libraries were generated. Paired-end reads (36 nt) were generated on an Illumina GAIIx. Reads were aligned to the genome using Efficient Large-Scale Alignment of Nucleotide Databases (ELAND), and reads mapping to SWI/SNF subunit genes were further analyzed. A custom C# script (available on request) was used to identify base substitutions and to identify paired reads and chimeric reads indicative of gene rearrangement. The complete RNAseq dataset for the pancreatic cancer cell lines will be detailed in a separate publication.

Functional Studies. For re-expression studies, retroviral expression constructs were obtained from Addgene: no. 1959 (SMARCA4), no. 1960 (SMARCA4-K798R), and no. 1964 (pBABE). Virus was produced in 293T cells using pVPack-GP (Agilent) and pMD2.g (VSV-G) (Addgene) packaging plasmids, and was then used to transduce target cell lines, which were selected and maintained with puromycin in RPMI-1640 media with 10% (vol/vol) FBS. For RNAi studies, HPDE cells were grown in keratinocyte serum-free media (supplemented with EGF and bovine pituitary extract, as noted) and HaCaT cells were grown in DMEM with 10% (vol/vol) FBS. ON-TARGETplus siRNA pools and the Non-Targeting pool were obtained from Dharmacon. A total of 50,000 cells were plated in six-well plate wells and then transfected (time 0) with 20 nM siRNA using Lipofectamine 2000 reagent (Invitrogen). The media were changed the following morning, and every 24 h thereafter. Cell growth/viability was quantified using the WST-1 reagent kit (Roche). Experiments were carried out in triplicate (as biological replicates), and all experiments were done at least twice. Cellular senescence was quantified by senescence-associated β-galactosidase staining (Millipore). For clonogenicity assays, cells were transfected with the above cDNA constructs and plated. Following 30 d of growth in puromycin, colonies ≥1 mm were counted. Antibodies used for Western blot analysis include ARID1A (H00008289-M01; Novus), ARID1B (H00057492-M01; Novus), PBRM1 (A301-591A; Bethly Laboratories), SMARCA2 (610389; BD Transduction Laboratories), SMARCA4 (10768; Santa Cruz), and GAPDH (sc-25778; Santa Cruz). Quantitative densitometry was done using ImageJ software (National Institutes of Health).

ACKNOWLEDGMENTS. We thank members of the J.R.P. laboratory for helpful discussions. This study was funded, in part, by National Cancer Institute Grant R01CA112016 (to J.R.P); by National Cancer Institute Grants P01CA134292, P50CA062924, and R01CA113669 (to A.M.); by a grant from the Lustgarten Foundation (to J.R.P.); and by a core grant (to M.D.B) to the Centre for DNA Fingerprinting and Diagnostics by the Department of Biotechnology, Government of India. M.D.B. was supported, in part, by a Biotechnology Overseas Associateship.

1. Parkin DM, Bray FI, Devesa SS (2001) Cancer burden in the year 2000. The global picture. *Eur J Cancer* 37(Suppl 8):S4–S66.
2. Jemal A, et al. (2009) Cancer statistics, 2009. *CA Cancer J Clin* 59:225–249.
3. Hidalgo M (2010) Pancreatic cancer. *N Engl J Med* 362:1605–1617.
4. Koorstra JB, Hustinx SR, Offerhaus GJ, Maitra A (2008) Pancreatic carcinogenesis. *Pancreatology* 8:110–125.
5. Hezel AF, Kimmelman AC, Stanger BZ, Bardeesy N, Depinho RA (2006) Genetics and biology of pancreatic ductal adenocarcinoma. *Genes Dev* 20:1218–1249.

6. Massagué J (2008) TGFbeta in Cancer. *Cell* 134:215–230.
7. PancreaticCancerStrategicPlanWorkgroup (2002) Strategic plan for addressing the recommendations of the pancreatic cancer progress review group. Available at *http://planning.cancer.gov/library/pancreatic.pdf*. Accessed September 7, 2011.
8. Jones S, et al. (2008) Core signaling pathways in human pancreatic cancers revealed by global genomic analyses. *Science* 321:1801–1806.
9. Bashyam MD, et al. (2005) Array-based comparative genomic hybridization identifies localized DNA amplifications and homozygous deletions in pancreatic cancer. *Neoplasia* 7:556–562.
10. Aguirre AJ, et al. (2004) High-resolution characterization of the pancreatic adenocarcinoma genome. *Proc Natl Acad Sci USA* 101:9067–9072.
11. Kimmelman AC, et al. (2008) Genomic alterations link Rho family of GTPases to the highly invasive phenotype of pancreas cancer. *Proc Natl Acad Sci USA* 105: 19372–19377.
12. Chen S, et al. (2008) Copy number alterations in pancreatic cancer identify recurrent PAK4 amplification. *Cancer Biol Ther* 7:1793–1802.
13. Kwei KA, et al. (2008) Genomic profiling identifies GATA6 as a candidate oncogene amplified in pancreatobiliary cancer. *PLoS Genet* 4:e1000081.
14. Fu B, Luo M, Lakkur S, Lucito R, Iacobuzio-Donahue CA (2008) Frequent genomic copy number gain and overexpression of GATA-6 in pancreatic carcinoma. *Cancer Biol Ther* 7:1593–1601.
15. Wood LD, et al. (2007) The genomic landscapes of human breast and colorectal cancers. *Science* 318:1108–1113.
16. Bignell GR, et al. (2010) Signatures of mutation and selection in the cancer genome. *Nature* 463:893–898.
17. Su GH, et al. (1998) Alterations in pancreatic, biliary, and breast carcinomas support MKK4 as a genetically targeted tumor suppressor gene. *Cancer Res* 58:2339–2342.
18. Wang X, et al. (2004) Two related ARID family proteins are alternative subunits of human SWI/SNF complexes. *Biochem J* 383:319–325.
19. Reisman D, Glaros S, Thompson EA (2009) The SWI/SNF complex and cancer. *Oncogene* 28:1653–1668.
20. Weissman B, Knudsen KE (2009) Hijacking the chromatin remodeling machinery: Impact of SWI/SNF perturbations in cancer. *Cancer Res* 69:8223–8230.
21. Wong AK, et al. (2000) BRG1, a component of the SWI-SNF complex, is mutated in multiple human tumor cell lines. *Cancer Res* 60:6171–6177.
22. Ouyang H, et al. (2000) Immortal human pancreatic duct epithelial cell lines with near normal genotype and phenotype. *Am J Pathol* 157:1623–1631.
23. de la Serna IL, Roy K, Carlson KA, Imbalzano AN (2001) MyoD can induce cell cycle arrest but not muscle differentiation in the presence of dominant negative SWI/SNF chromatin remodeling enzymes. *J Biol Chem* 276:41486–41491.
24. Lee D, et al. (2002) SWI/SNF complex interacts with tumor suppressor p53 and is necessary for the activation of p53-mediated transcription. *J Biol Chem* 277: 22330–22337.
25. Hill DA, de la Serna IL, Veal TM, Imbalzano AN (2004) BRCA1 interacts with dominant negative SWI/SNF enzymes without affecting homologous recombination or radiation-induced gene activation of p21 or Mdm2. *J Cell Biochem* 91:987–998.
26. Cheng SW, et al. (1999) c-MYC interacts with INI1/hSNF5 and requires the SWI/SNF complex for transactivation function. *Nat Genet* 22:102–105.
27. Boukamp P, et al. (1997) Sustained nontumorigenic phenotype correlates with a largely stable chromosome content during long-term culture of the human keratinocyte line HaCaT. *Genes Chromosomes Cancer* 19:201–214.
28. Xi Q, He W, Zhang XH, Le HV, Massagué J (2008) Genome-wide impact of the BRG1 SWI/SNF chromatin remodeler on the transforming growth factor beta transcriptional program. *J Biol Chem* 283:1146–1155.
29. Isakoff MS, et al. (2005) Inactivation of the Snf5 tumor suppressor stimulates cell cycle progression and cooperates with p53 loss in oncogenic transformation. *Proc Natl Acad Sci USA* 102:17745–17750.
30. Tie F, Furuyama T, Prasad-Sinha J, Jane E, Harte PJ (2001) The Drosophila Polycomb Group proteins ESC and E(Z) are present in a complex containing the histone-binding protein p55 and the histone deacetylase RPD3. *Development* 128:275–286.
31. van der Vlag J, Otte AP (1999) Transcriptional repression mediated by the human polycomb-group protein EED involves histone deacetylation. *Nat Genet* 23:474–478.
32. Simon JA, Lange CA (2008) Roles of the EZH2 histone methyltransferase in cancer epigenetics. *Mutat Res* 647:21–29.
33. Wilson BG, et al. (2010) Epigenetic antagonism between polycomb and SWI/SNF complexes during oncogenic transformation. *Cancer Cell* 18:316–328.
34. Roberts CW, Orkin SH (2004) The SWI/SNF complex—Chromatin and cancer. *Nat Rev Cancer* 4:133–142.
35. Rosson GB, Bartlett C, Reed W, Weissman BE (2005) BRG1 loss in MiaPaCa2 cells induces an altered cellular morphology and disruption in the organization of the actin cytoskeleton. *J Cell Physiol* 205:286–294.
36. Birnbaum DJ, et al. (2011) Genome profiling of pancreatic adenocarcinoma. *Genes Chromosomes Cancer* 50:456–465.
37. Wiegand KC, et al. (2010) ARID1A mutations in endometriosis-associated ovarian carcinomas. *N Engl J Med* 363:1532–1543.
38. Jones S, et al. (2010) Frequent mutations of chromatin remodeling gene ARID1A in ovarian clear cell carcinoma. *Science* 330:228–231.
39. Varela I, et al. (2011) Exome sequencing identifies frequent mutation of the SWI/SNF complex gene PBRM1 in renal carcinoma. *Nature* 469:539–542.
40. Kennison JA, Tamkun JW (1988) Dosage-dependent modifiers of polycomb and antennapedia mutations in Drosophila. *Proc Natl Acad Sci USA* 85:8136–8140.
41. Kennison JA (1995) The Polycomb and trithorax group proteins of Drosophila: Trans-regulators of homeotic gene function. *Annu Rev Genet* 29:289–303.
42. Tamkun JW, et al. (1992) brahma: A regulator of Drosophila homeotic genes structurally related to the yeast transcriptional activator SNF2/SWI2. *Cell* 68:561–572.
43. Rubio-Viqueira B, et al. (2006) An in vivo platform for translational drug development in pancreatic cancer. *Clin Cancer Res* 12:4652–4661.
44. Beroukhim R, et al. (2007) Assessing the significance of chromosomal aberrations in cancer: Methodology and application to glioma. *Proc Natl Acad Sci USA* 104: 20007–20012.
45. Reich M, et al. (2006) GenePattern 2.0. *Nat Genet* 38:500–501.